Closed-Loop Control of a Wing in an Unsteady Flow

David Williams[1], Wesley Kerstens[2], Seth Buntain[2] and Vien Quach[2]
Illinois Institute of Technology, Chicago, IL, 60616

Jens Pfeiffer[3], Rudibert King[4]
Technische Universität Berlin, Berlin,Germany

Gilead Tadmor[5]
Northeastern University, Boston, MA, 02115,

and

Tim Colonius[6]
California Institute of Technology, Pasadena, CA, 91125

The lift response of the separated flow over a wing to different actuator input disturbances is used to obtain linear models useful for closed-loop control design. The wing has a small aspect ratio, a semi-circular planform, and is fully stalled at a 20^o angle of attack. Individual pulse-like disturbances and step-input disturbances with randomized frequency were inputs to the actuator, and the lift coefficient increments were output signals. The "prediction error method" system identification technique was used to obtain two linear models of the separated flow. A 4^{th} order model reproduced the non-minimum phase behavior of the pulse input, but did not work well for control purposes. The second model identified was limited to first order. The first order model proved to be useful for designing a proportional-integral feedback controller capable of suppressing lift oscillations in unsteady flows. Good suppression of lift oscillations was observed in the experiment after a step change in wind tunnel flow speed occurred. When the control system was tested with a randomized freestream velocity, it reduced the root-mean-square lift oscillation by 50 percent relative to the uncontrolled case.

Nomenclature

C_L = lift coefficient of wing
C_{Lref} = reference lift coefficient used for control
$C\mu$ = momentum coefficient, $= \dfrac{\rho U_{jet}^2 h}{0.5\rho U^2 c}$
c = chord
k = normalized frequency, $\pi fc/U$
q = dynamic pressure, $0.5\,\rho U^2$
Re = Reynolds number based on chord, $\rho Uc/\mu$
S = planform area, m^2
St = fc/U
t = time, sec
t^+ = dimensionless time tU/c.

[1] Professor, Mechanical and Aerospace Engineering Department, and AIAA Associate Fellow.
[2] Graduate Research Assistant, Mechanical and Aerospace Engineering Department, and AIAA Student Member.
[3] Graduate Research Assistant, Measurement and Control Group
[4] Professor, Measurement and Control Group, and AIAA Member.
[5] Professor, Electrical and Computer Engineering Department, and AIAA Member.
[6] Professor, Mechanical Engineering Department, and AIAA Associate Fellow.

t_{conv} = convective time, c/U
U' = longitudinal velocity increment, m/s
U = wind tunnel freestream speed, m/s
α = angle of attack, degrees
φ = phase lag between actuator input signal and the lift force, degrees
τ^+ = normalized time delay, $t_{delay}U/c$

I. Introduction

The analysis of conventional flight control in gusting flows considers only the long-time averaged statistical properties of the flow unsteadiness[1]. If the control system is somehow able to react to instantaneous changes in flow speed and direction associated with gusts, then it may be possible to fly in a way that extracts some energy from the gusts. With proper application of active flow control techniques, it may be possible to realize significant range and endurance enhancements in flight vehicles that use real-time control of the vehicle in response to flow unsteadiness. Real-time control of flight through unsteady and gusting flows requires control systems that account for both the unsteady aerodynamics and the flow system response to the actuator. Quasi-steady models are usually not sufficient for closed loop control when the flight vehicle response is expected to be faster than k >0.05, because of the time lags and amplitude changes associated with both the unsteady aerodynamics and the actuator response. In this paper the focus is on the latter.

Previous measurements of the transient flow response to actuation [2-6] have shown relatively long time delays in the flow response to the onset of actuation. Normalized time delays τ^+=5.3 were measured for response to sinusoidal inputs from the actuator [7]. Phase lags between the freestream speed oscillation and the lift force were measured to be $\varphi = 30^o$ at k = 0.2. These are large delays, and an effective controller must be able to quickly compensate for these time delays and for changes in amplitude associated with the flow disturbances.

Figure 1. Wind tunnel test section showing the semi-circular wing model mounted on its sting. Flow is from left to right. Flow unsteadiness is created by the shutter system at the downstream end of the test section.

In an earlier study [7], the ability of a simple feed-forward controller to suppress the lift force fluctuations produced by a sinusoidally oscillating freestream flow was demonstrated. However, that control approach was limited to a specific frequency of oscillation. The controller required manual changes in amplitude and phase delay in order to account for any frequency or amplitude changes. A more general approach is to use a system model that contains the amplitude and phase information of the lift coefficient response to actuation over a wide band of operating conditions.

Because the wing is in a fully stalled state with a fixed $\alpha = 20^o$, one might expect nonlinear behavior to dominate the response to actuation. The use of neural networks or look-up tables as nonlinear models is an option for the control approach. However, pulse response experiments [7, 8] indicate that linear models can be used effectively within certain limitations. A linear system model can almost always be obtained, but the question is over what range of conditions will it be valid? An equally important question is given a linear model of the system, can a useful controller be designed? We investigate these questions using experimental data to obtain black-box system models, and using conventional linear controller design techniques.

In the following sections, the use of system identification techniques to obtain two linear models which approximate the separated flow response to actuator input disturbances is obtained. The first model is a higher order which is compared to the pulse response results. A second lower order model is then obtained using similar system identification techniques, which acts as a plant model for the design of a standard proportional-integral (PI) controller. The ability of the feed forward, PI-controller to maintain a constant lift force is tested with randomized "step changes" in the freestream speed of the wind tunnel. In Section V the idealized models are used to speculate about the possible improvements in system response that can be achieved with closed loop flow control.

II. Experimental Setup

The experiments were conducted in the Andrew Fejer Unsteady Flow Wind Tunnel at the Illinois Institute of Technology. Figure 1 shows the wind tunnel test section with the model mounted on its sting. The test section dimensions are 610 mm by 610 mm with a length of 3,100 mm. The wind tunnel is capable of speeds up to 30 m/s, but for the purpose of this experiments speeds ranged from 3 m/s to 9 m/s. The highest level of freestream turbulence level was measured to be 0.6 percent at an average speed of 3 m/s and over a bandwidth from 0.1 Hz to 30 Hz. The freestream turbulence levels were inversely proportional to the average flow speed.

The wing has a semi-circular planform with the circular part forming the leading edge and the straight part forming the trailing edge. The center-span wing chord is c =0.203m and the planform area S = 0.065m^2. The leading edge is tapered with a 5:1 elliptic shape, and the thickness to chord ratio is 0.069. The centerline based chord Reynolds numbers ranged from Re_c = 47,000 to 140,000. The wing was constructed from Duraform® nylon using a 3D Systems, Inc. selective laser sintering, rapid prototyping machine. The wing was fixed at angle of attack α=20^o for all of the measurements in this study. The flow was fully separated. At α=20^o angle of attack the blockage area ratio is 6 percent. No corrections for blockage were made to the data.

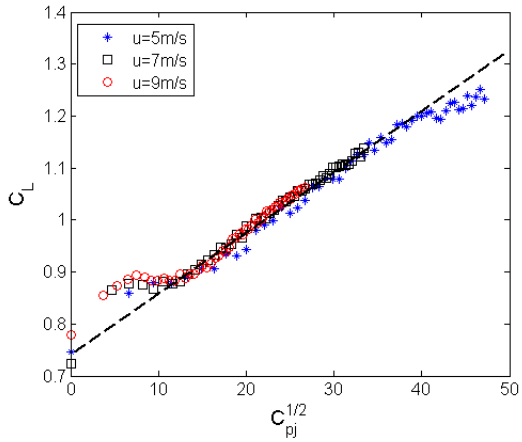

Figure 2. Static map – lift coefficient dependence on the actuator supply pressure coefficient. Then angle of attack is fixed at α = 20^o and the actuators are pulsed continuously at 29 Hz.

In previous studies [9-11] the ability of pulsed-blowing jets to modify the flow around the leading edge and wing tips on low aspect ratio wings was demonstrated. The pulsed-blowing actuation system consists of a regulated air supply, a plenum inside the wing, and 16 Lee, Inc. micro-valves designed to fit into the leading edge of the wing. The flow rates were measured with the actuator micro-valves continuously pulsing at 29 Hz. With actuator supply pressures of 6.9 kPa (1 psi), 20.7 kPa (3 psi), and 34.5 kPA (5 psi) the average flow rates are 1.91x10^{-4} kg/s, 3.35x10^{-4} kg/s, and 9.26x10^{-4} kg/s, respectively. For reference purposes, continuous actuation at 29Hz, U = 5m/s and a supply pressure of 34.5 kPa corresponds to an average C_μ = 0.0074.

For transient experiments the valve-open time was set at 0.017 seconds, corresponding to the 29 Hz case. The valves were controlled by a PC-based data acquisition system using a National Instruments 16-bit A/D converter and software written with Mathworks Data Acquisition Toolbox. The sampling rate was 1000 samples per second, giving an uncertainty of +/- .0005 seconds for the pulse time interval. The supply pressure to the plenum inside the wing is controlled by a Fairchild TA 6000 pneumatic transducer, which had an approximate bandwidth estimated to be 2 Hz.

The forces and moments acting about the three principal axes on the wing were recorded with a 6-component balance (ATI, Inc. - Nano 17). The uncertainty in the force measurement was based on the repeatability of calibration data and was estimated to be ±0.05 N.

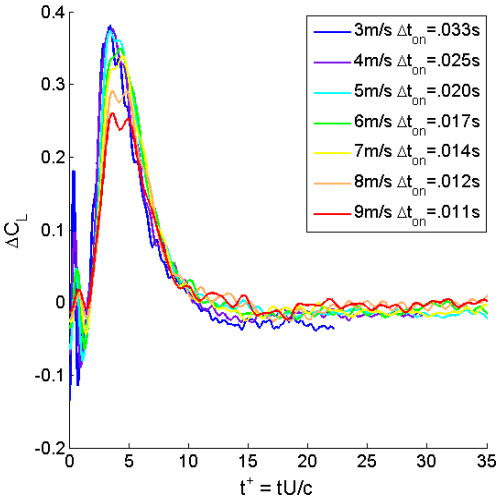

Figure 3. Phase-averaged lift response to single-pulse disturbances from the pulse-jet actuator. Seven different free stream speeds and valve-open times were varied in a way to keep $U\Delta t_{on}$ = constant, while the actuator supply pressure was kept constant at 34.5 kPa.

The earlier measurements with the static wing [7] showed that without flow control the wing stalls at 15^o angle of attack, and the maximum lift coefficient is C_{Lmax} = 0.9. At α =20^o the lift coefficient decreases to C_L = 0.75. With continuously pulsing active flow control, the wing stall angle is delayed to α =23^o and a higher maximum lift

coefficient occurs, C_{Lmax} = 1.3. By fixing the wing at α =20^o the open loop controlled actuator can vary the lift coefficient from C_L =0.75 to C_L =1.25.

III. Controller Design

The controller design methodology used by Henning, et al.[12] to reduce the drag behind bluff bodies was followed in this experiment. First, the open-loop response of the lift coefficient to different actuator supply pressures was documented to obtain the static response map as shown in Fig.2. Next, the dynamic response of the lift coefficient was measured using open-loop, pulsed and randomized step inputs to the pulsed-blowing actuators. A linear 'black-box' (input-output) model was obtained from the experimental data using conventional system identification techniques. With a linear model of the system dynamics, it was possible to use a variety of control design tools. For this experiment a feed forward controller supplemented with a proportional-integral (PI) feedback loop was chosen as the control architecture. Details about each of the steps are described below, and the results of the controller performance are given in the Section IV.

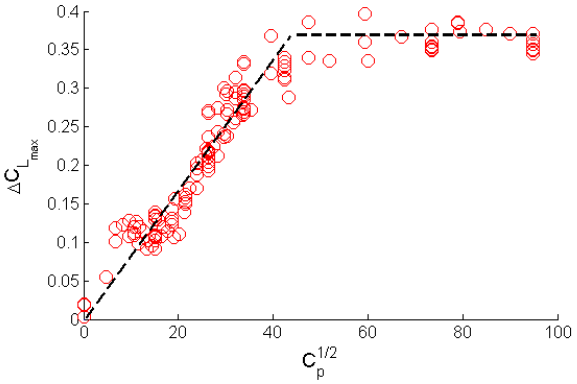

Figure 4. The peak in the transient lift coefficient dependence on actuator pressure coefficient. The actuator supplied only a single pulse with different supply pressures, flow speeds and valve open times.

A. Static response map

Without actuation the flow is separated over the suction surface of the wing, and the separation bubble closes some distance downstream of the trailing edge. With continuously pulsing actuation (at 29 Hz, St = fc/U= 0.65 – 1.2 over U = 5 m/s to 9 m/s) the separated flow reattaches on the top surface of the wing, and the lift coefficient is increased as shown in Fig. 2. At lower supply pressures the lift coefficient increase is essentially linear with the square root of the actuator supply pressure. Eventually a saturation point is reached near $C_{pj}^{0.5}$~40, beyond which further increases in actuation supply pressure do not change the increment in lift coefficient.

The saturated state obtained with continuous forcing is one steady state limit, just as the naturally occurring separated flow (without actuation) is a different steady state limit. The control system is designed to work between the no forcing limit and the 29 Hz continuous pulsing limit.

As a side note, continuous blowing (not pulsed) from the actuators creates a third steady state that is different from the other two. However, the steady blowing reduces the lift coefficient to a value lower than the unforced case, so it is not of interest in this experiment.

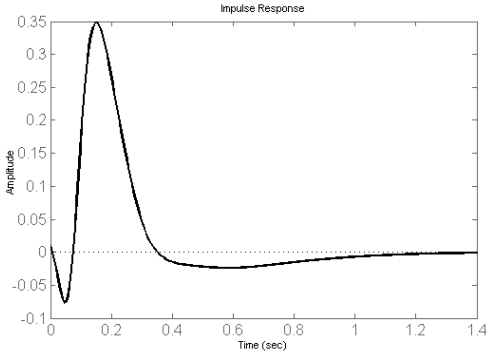

Figure 5. Impulse response of the system-ID model obtained from the data in Fig. 3.

B. Dynamic response to actuation

For gust suppression purposes the controller is designed to maintain a constant reference *lift force* when the free stream speed is varied. This means the corresponding reference *lift coefficient* will change inversely with the dynamic pressure. For low frequency oscillations in the free stream speed, such as, k<0.05, a quasi-steady controller based solely on the static map in Fig. 2 might be sufficient to maintain a constant lift force. But at higher frequency oscillations the static map does not provide a sufficiently accurate model of the system dynamics, because of the time lags and amplitude changes that cause the lift to deviate from the static map. The procedure for obtaining a dynamic model of the system is described next.

Two 'black box' models of the open-loop system dynamics were obtained from the experimental data using the prediction error method. The first used single, short-time pulses approximating an impulse. The second used pseudo-random step input changes to the supply pressure coefficient. In both cases the measured lift coefficient was the output.

B.1. Model obtained from pulse inputs

The time varying increment in the lift coefficient response to different pulse-like disturbances is shown in Fig. 3. The time axis is scaled by the convective time, $t_{conv} = c/U$. Different freestream speeds and valve open times were combined to keep the dimensionless valve open time constant, $U\Delta t_{on}/c = 0.49$. The peak in the transient lift coefficient is plotted in Fig. 4 for a wide range of flow speeds, supply pressures and valve open times. It is interesting that the transient peak amplitude shows the same trends as the continuously pulsed actuation shown in Fig 2. Saturation occurs in both cases when the supply pressure coefficient exceeds $[C_{pj}]^{0.5} > 40$.

For the data shown in Fig. 3 the actuator supply pressure was kept constant. The reduction in the peak values occurring at higher flow speeds 7 – 9m/s are the result of the corresponding lower values of C_{pj}. As the freestream speed increases, the supply pressure coefficient decreases, and the peak lift coefficient is no longer saturated.

A 4th order model was identified from the pulse response data with a 34.5 kPa supply pressure, similar to the data shown in Fig. 3. The impulse response predicted by that model is shown in Fig. 5. The impulse response captures the initial decrease in C_L (non-minimum phase behavior) at the beginning of the transient. Similar behavior was seen by other investigators [2-5] studying transient responses to actuation.

The phase between the output lift coefficient and input actuator signal is compared in Fig. 6. The model prediction is in reasonable agreement with the experimentally measured values.

Although the dynamics appeared to be accurately modeled with the 4th order model, our initial attempts at designing a controller did not result in satisfactory results. It was hypothesized that the 4th order model might be modeling system noise, so a lower order (1st order) model was sought as described in the next section.

B.2. Model obtained from pseudo-random step inputs

Instead of using pulse-like inputs to the actuator, a sequence of pseudo-random step inputs were applied to the supply pressure of the actuator. The times between the steps and the duration of the steps were varied from 1s to 4s in a pseudo-random manner. Five different models were obtained for different actuator supply pressures. Different step amplitudes were used to create a family of response curves that covered the linear

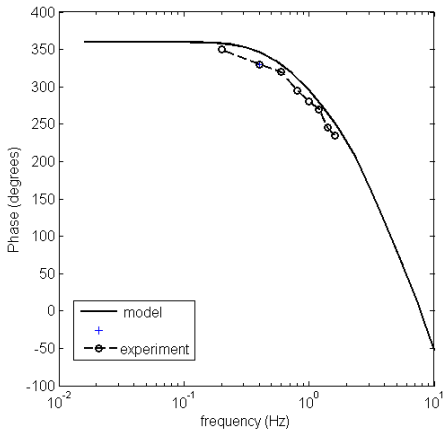

Figure 6. Phase dependence from system ID model compared with experimentally measured phase.

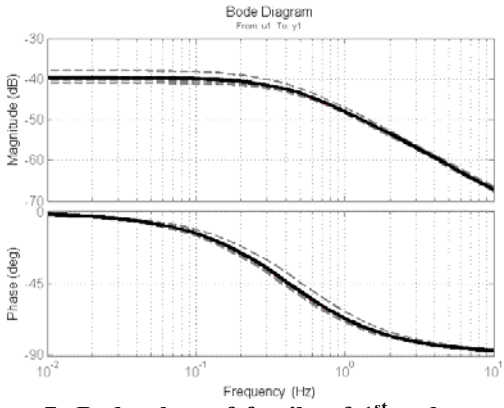

Figure 7. Bode plots of family of 1st order system models and the nominal model (heavy line) used for control design purposes.

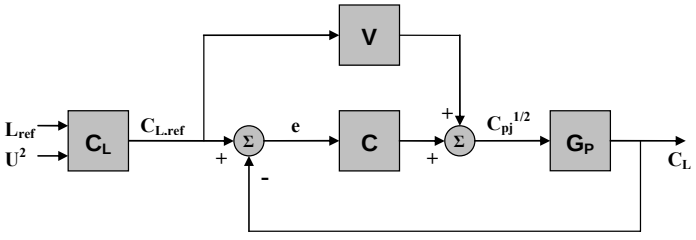

Figure 8. Block diagram of feed forward control (V) and PI feedback control (C).

operating range on the static response map shown in Fig. 2. The family of models is shown in Bode plot form in Fig. 7. The dashed lines show the individual models identified for each supply pressure. The mean of the parameters from the identified models was calculated to form the 'nominal system model', which is representative of the family as shown by the heavy line. The nominal model was used in the controller design process described next.

C. Feed forward and PI control architecture

The control architecture schematic is shown in Fig. 8. The plant model uses $C_{pj}^{0.5}$ as input and C_L as output. Because the control objective is to maintain a constant lift, L_{ref}, the control problem becomes one of tracking a desired lift coefficient, C_{Lref}, which is changing as the freestream speed changes. The instantaneous freestream speed is measured using a constant temperature hot wire anemometer. The flow speed is converted to dynamic pressure and used to compute C_{Lref}. A feed forward controller (V) is added to speed up the reference tracking. The feed forward controller is obtained from the inverse of the nominal plant transfer function combined with a filter that is needed to maintain causality. The proportional integral controller (C) is designed using Mathworks™ 'sisotool' graphical user interface. The lift coefficient output from the plant, C_L, is fed back and compared to the reference lift coefficient to obtain an error signal, which is input to the PI controller.

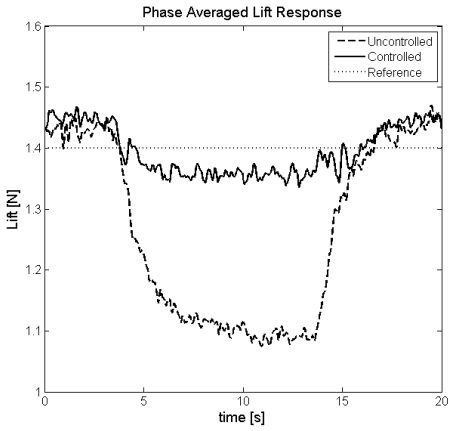

Figure 9. Lift response of the wing to step changes in freestream flow speed. Uncontrolled case – dashed line; controlled case – solid line; reference lift – dotted line.

IV. Results

A. Proportional Integral Feedback Control

The ability of the controller to maintain a constant lift when the freestream speed of the tunnel undergoes step changes with a 10 s period in flow speed is shown in Fig. 9. The reference lift was set at 1.4 N. The freestream speed was controlled by step inputs to the shutter. Initially the speed is set at 7 m/s, and then a "step-down" to 6.2 m/s is produced by closing the shutter mechanism in the wind tunnel. Ten seconds later the flow is accelerated through a "step-up" maneuver from 6.2 m/s to 7.0 m/s. The inertia of the flow in the wind tunnel requires more than two seconds for the deceleration and acceleration of the flow to occur, which is a relatively slow maneuver relative to the bandwidth of the controller. Without control the lift drops by 30 percent from 1.45 N to 1.1 N when the flow speed decreases. With control the lift decreases to 1.36 N, which is a 7 percent drop. The controller is not compensating for the lift overshoot at 1.45 N.

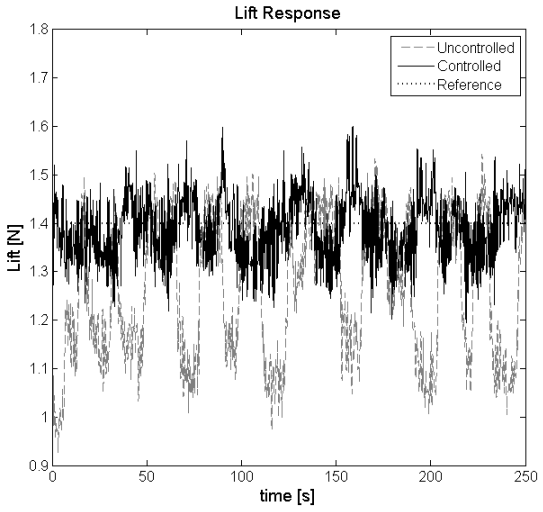

Figure 10. Lift response of the wing to randomized step changes in freestream flow speed. Uncontrolled case – light dashed line; controlled case – solid line; reference lift is 1.4 N – dotted line.

A more rigorous test of the control system is to use randomized changes in freestream speed amplitude and frequency. The results shown in Fig. 10 compare the cases with and without control. The reference lift value was set to 1.4 N. As in the previous case there is an overshoot of 0.05 N that is not compensated by the controller. This may be related to the 0.05 N uncertainty in the force measurement system, combined with the fact that the controller is not capable of reducing the lift below its unforced value. Nevertheless, the controller reduces the root mean square lift fluctuations by 50 percent relative to the uncontrolled case.

Although there is still room for improvement from the controller, the results demonstrate the feasibility of the linearized model approach to developing controllers that are effective in gust suppression. The 1st order model

captured important dynamics of the separated flow system and reduced the lift oscillations on the time scale of the current experiment.

V. Discussion of Results

The open loop transient lift response to a pulse-like disturbance from the actuator requires more than 10 convective time units to return to the undisturbed state as shown in Fig. 3. The question is often asked if the time scale of the transient response is a lower limit on the time response for active flow control of a flight vehicle? In fact, this question illustrates just how closed loop control is fundamentally different from open-loop control. The dynamics of a linear system can only be changed using closed loop control. It is possible to obtain a faster time response from the closed loop system than is possible with open loop control, provided one has a fast actuator and stable controller. To illustrate this point, the Bode plots for the idealized plant and controller are shown next.

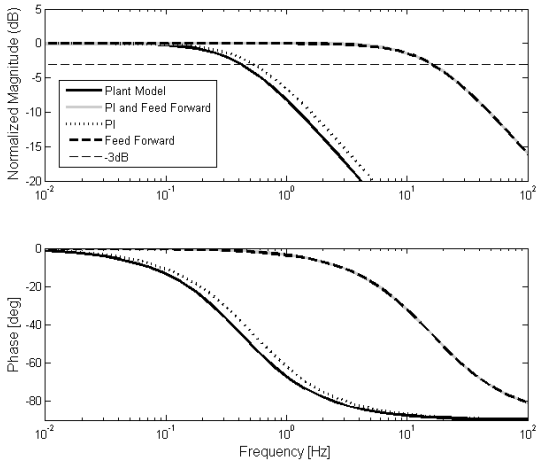

Figure 11. Open loop plant model – solid black line; feed forward only – dashed black line; PI control only – dotted line; combined PI and feed forward – light gray line overlays the feed forward only line.

The closed loop transfer function between the reference lift coefficient and the lift coefficient can be written as:

$$\frac{C_L(s)}{C_{L,ref}(s)} = \frac{C(s)G(s) + V(s)G(s)}{1 + C(s)G(s)}$$

Setting *V(s)*=0 yields the closed loop transfer function for PI control only, and setting *C(s)*=0 yields the transfer function from the reference lift coefficient to lift coefficient for feed forward control only. Fig. 11 shows the Bode plot comparison between the plant model, closed loop with PI and feed forward, closed loop with PI only and feed forward only. The feed forward control is dominant in determining the time response. The differences between the feed forward only control and the closed loop with PI and feed forward control are minimal.

The open loop case is simply the nominal 1st order system identification model obtained from the experimental data. The -3dB cutoff frequency is approximately 0.5Hz. By adding the feed forward component to control the cutoff frequency is increased to approximately 15 Hz. Again, it is emphasized that this is an idealized case. The unsteady aerodynamic effects, which have not been modeled would be important. Furthermore, the bandwidth of the current actuator is only 2 Hz. The purpose of the comparison is to illustrate that closed loop system responses significantly faster than with open-loop control can be achieved. In addition, the idealized results suggest significant performance enhancements can be achieved with higher bandwidth actuators.

VI. Conclusions

In the present experiment, the control objective was to suppress changes in lift force associated with changes in the freestream flow speed in an unsteady wind tunnel. Some benefits of using a linearized system models were demonstrated within the range of model validity. The static and transient lift coefficient response showed a square root dependence on the actuator supply pressure coefficient. System identification techniques were used to obtain two black box models of the separated flow over a fully stalled wing. The higher order model captured important features of the transient lift response to pulsed actuation, but did not produce a useful controller. The lower order (1st order) model of the system was the simplest, but it appeared to capture sufficient dynamics to allow the design of a closed-loop controller capable of suppressing lift oscillations. The r.m.s. lift oscillations were reduced by 50 percent when a randomized freestream speed and amplitude were applied to the wing.

More sophisticated control approaches are currently being explored, such as, modern robust controllers designed based on a more extensive family of linear models. Efforts are being made to increase the actuator bandwidth in order to test the 'predictions' of the system models described above.

Acknowledgments

The support for this work by the U.S. Air Force Office of Scientific Research MURI (FA9550-05-0369) with program manager Dr. Fariba Fahroo and contract FA9550-09-1-0189 with program manager Dr. Doug Smith is gratefully appreciated. David Williams gratefully acknowledges the partial support of the Alexander von Humboldt foundation. We also acknowledge the support from the Illinois NASA Space Grant Consortium for Wesley Kerstens and Seth Buntain.

References

[1] Hoblit, F.M., *Gust Loads on Aircraft: Concepts and Applications*, AIAA Education Series, Washington D.C., 1988.

[2] Darabi, A., and Wygnanski, I., "Active management of naturally separated flow over a solid surface. Part 1. The forced reattachment process," J. Fluid Mech., Vol. 510, 2004, pp. 105-129.

[3] Darabi, A., and Wygnanski, I., "Active management of naturally separated flow over a solid surface. Part 2. The separation process," J. Fluid Mech., Vol. 510, 2004, pp. 131-144.

[4] Brzozowski, D., and Glezer, A., "Transient Separation Control using Pulse-Combustion Actuation," AIAA Paper 2006-3024.

[5] Amitay, M., and Glezer, A., "Controlled Transients of Flow Reattachment over Stalled Airfoils," Int. J. of Heat Transfer and Fluid Flow, Vol. 23, 2002, pp. 690-699.

[6] Williams, D., Tadmor, G., Colonius, T., Kerstens, W., Quach, V., Buntain, S., "The lift response of a stalled wing to pulsatile disturbances," AIAA. J., Vol. 47, No. 12, 2009, pp.3031-3037.

[7] Williams, D.R., Quach, V., Kerstens, W., Buntain, S., Tadmor, G., Rowley, C., Colonius, T. "Low-Reynolds Number Wing Response to an Oscillating Freestream with and without Feed Forward Control," AIAA Paper 2009-143.

[8] Woo, G.T.K., Crittenden, T.M., and Glezer, A., "Transitory Control of a Pitching Airfoil using Pulse Combustion Actuation," 4th Flow Control Conference, AIAA Paper 2008-4324, June 2008.

[9] Williams, D.R., Doshi, S., Collins, J., Colonius, T., "Control of the Spanwise Distribution of Circulation on NACA 0012 and Flat Plate Wings," AIAA Paper 2007-1121.

[10] Colonius, T., Rowley, C.W., Tadmor, G., Williams, D.R., Taira, K., "Closed-loop Control of leading-edge and tip vortices for small UAV," 1st Conference on Active Flow Control, Berlin Germany, Sept. 27-29, 2006.

[11] Williams, D., Collins, J., Jankhot, C., Colonius, T., and Tadmor, G., "Control of Flow Structure on a Semi-Circular Planform Wing," AIAA Paper 2008-0597.

[12] Henning, L., Pastoor, M., King, R., Noack, B., and Tadmor, G., "Feedback control applied to the bluff body wake," R. King (Ed.): Active Flow Control, NNFM 95, Springer-Verlag, 2007, pp. 369-390.